Materials Research Bulletin 91 (2017) 31–35

Contents lists available at ScienceDirect

Materials Research Bulletin

journal homepage: www.elsevier.com/locate/matresbu

Electrocaloric effect in Pb-free Sr-doped $BaTi_{0.9}Sn_{0.1}O_3$ ceramics

Shuang Qi[a], Ganghua Zhang[b], Linhai Duan[a,*], Tao Zeng[b,*], Jianwu Cao[c]

[a] Key Laboratory of Petrochemical Catalytic Science and Technology, Liaoning Shihua University, Fushun 113000, China
[b] Shanghai Key Laboratory of Engineering Materials Application and Evaluation, Shanghai Research Institute of Materials, 99 Handan Road, Shanghai 200437, China
[c] Beijing Institute of Technology, 5 South Venue of Zhongguan Village, Beijing 100086, China

ARTICLE INFO

Article history:
Received 3 November 2016
Received in revised form 5 February 2017
Accepted 13 March 2017
Available online 18 March 2017

Keywords:
Electrocaloric effect
Lead-free
Sr dopant

ABSTRACT

Perovskite-type $Ba_{1-x}Sr_xTi_{0.9}Sn_{0.1}O_3$ ($x = 0$, 0.06, 0.07, and 0.08) oxides were prepared by conventional solid-state synthesis, and their electrocaloric effect was investigated, revealing that doping by Sr reduces the Curie temperature to ambient values. The largest electrocaloric strength of 0.31 K mm kV^{-1} was obtained for $x = 0.06$ at 47 °C, significantly exceeding values displayed by other lead-free ceramics and implying that novel Sr-doped $Ba_{1-x}Sr_xTi_{0.9}Sn_{0.1}O_3$ ceramics are promising materials for ecofriendly refrigeration applications.

1. Introduction

In the past decades, materials exhibiting the electrocaloric effect (ECE) have attracted considerable interest due to their potential applications in solid-state cooling devices [1,2], helping to achieve higher energy efficiency and lower cost [3]. The ECE is defined as the reversible temperature change (ΔT) or isothermal entropy change of a dielectric material when an external electric field (ΔE) is applied or removed [4], with the cooling or heating capacity of materials [5] usually evaluated in terms of electrocaloric strength ($\Delta T/\Delta E$). Up to now, extensive efforts have been directed at developing materials with enhanced ECE [6], e.g., lead-based materials such as $PbZr_{0.95}Ti_{0.05}O_3$ thin films [7] ($\Delta T = 12$ K at 226 °C, $\Delta E = 48$ kV mm^{-1}, $\Delta T/\Delta E = 0.25$ K mm kV^{-1}), $Pb_{0.97}La_{0.02}(Zr_{0.75}Sn_{0.18}Ti_{0.07})O_3$ thick films [8] ($\Delta T = 53.8$ K at 5 °C, $\Delta E = 90$ kV mm^{-1}, $\Delta T/\Delta E = 0.598$ K mm kV^{-1}), and PMN-PT ceramics [9] ($\Delta T = 0.558$ K at 70 °C, $\Delta E = 2.4$ kV mm^{-1}, $\Delta T/\Delta E = 0.233$ K mm kV^{-1}). However, these Pb-doped electrocaloric materials are harmful to the environment, necessitating the development of lead-free electrocaloric materials for environment-friendly solid-state cooling devices. A number of lead-free high-ECE materials have been discovered so far, such as polyvinylidene fluoride–trifluoroethylene [P(VDF-TrFE)] thin films [10] ($\Delta T = 12$ K at 80 °C, $\Delta E = 209$ kV mm^{-1}, $\Delta T/\Delta E = 0.057$ K mm kV^{-1}), $Ba_{0.65}Sr_{0.35}Ti_{0.997}Mn_{0.003}O_3$ ceramic [11] ($\Delta T = 3.1$ K at 20 °C, $\Delta E = 13$ kV mm^{-1}, $\Delta T/\Delta E = 0.238$ K mm kV^{-1}), and 0.6BZT–0.4BCT ceramic [12] ($\Delta T = 0.58$ K at 125 °C, $\Delta E = 2.8$ kV mm^{-1}, $\Delta T/\Delta E = 0.207$ K mm kV^{-1}).

Among lead-free materials, prototypical lead-free barium titanate (BTO)-based compounds have been widely studied [13–15] due to their advantageous electromechanical properties. On the other hand, maximal ECE can be obtained at temperatures close to that of the ferroelectric–paraelectric (FE–PE) phase transition (Curie temperature, T_c), which usually lies far above room temperature [6,16,17]. Thus, to fulfill the requirements of practical applications, the Curie temperature of electrocaloric materials should be adjusted to room temperature. Recently, numerous studies have focused on lowering T_c by chemical substitution. For example, Sn-doped $BaTiO_3$ ceramics [18,19] exhibited a large ECE ($\Delta T = 0.61$ K, $\Delta E = 2.0$ kV mm^{-1}, $\Delta T/\Delta E = 0.305$ K mm kV^{-1}) at 28 °C for $BaTi_{0.895}Sn_{0.105}O_3$ ceramics, but the temperature is different from our results and those reported previously [19]. In addition, since the ECE is a reversible manifestation of pyroelectric properties, it is presumably large for Ba–Sr–Ti–O systems, where these properties are very pronounced [20–22]. Therefore, Sr-doped $BaTi_{1-x}Sn_xO_3$ may be explored as new lead-free electrocaloric materials with excellent ECE. In this study, $Ba_{1-x}Sr_xTi_{0.9}Sn_{0.1}O_3$ ($x = 0$, 0.06, 0.07, and 0.08) ceramics were prepared by conventional solid-state synthesis, and the influence of Sr content on their dielectric, ferroelectric, and electrocaloric properties was investigated.

2. Experimental

$Ba_{1-x}Sr_xTi_{0.9}Sn_{0.1}O_3$ ($x = 0$, 0.06, 0.07, and 0.08) ceramics were prepared from $BaCO_3$ (99%), $SrCO_3$ (99%), TiO_2 (99%), and SnO_2

* Corresponding authors.
E-mail addresses: lhduan@126.com (L. Duan), 18341310503@163.com (T. Zeng).

http://dx.doi.org/10.1016/j.materresbull.2017.03.026
0025-5408/

(99.5%) powders by conventional solid-state synthesis. Ceramic samples were prepared by calcining mixtures of ground powders (weighed in a certain stoichiometric ratio) at 1150 °C for 4 h. After grinding and granulating, the calcined powders were pressed into 15 mm diameter pellets and sintered at 1380 °C for 4 h in a covered alumina crucible, and the thus obtained ceramics were polished to 1 mm thickness. For electrical measurements, silver electrodes were painted on both surfaces of ceramic samples. The crystal structure and phase purity of the above samples were confirmed by powder X-ray diffraction (XRD, D/MAX-2550 V, Rigaku, Tokyo, Japan). Dielectric constants were determined using a Hewlett-Packard LCR meter (Hewlett-Packard, Kobe-shi, Japan), and ferroelectric hysteresis loops were recorded at 1 Hz and a stabilization time of 15 min using an aix ACCT TF Analyzer 2000 instrument (aix ACCT Co., Aachen, Germany).

3. Results and discussion

Room-temperature powder XRD patterns of $Ba_{1-x}Sr_xTi_{0.9}Sn_{0.1}O_3$ ($x = 0$, 0.06, 0.07, and 0.08) are shown in Fig. 1. All Bragg peaks could be indexed to the known perovskite crystal structure of $BaTiO_3$ [23] and were refined by the Rietveld method. The ceramic products crystallized in the tetragonal system (space group *P*4*mm*), with the corresponding crystallographic parameters listed in Table 1. As shown in the above table, the unit cell volume decreases with increasing strontium content, confirming the formation of a solid solution as a result of Sr doping. The observed lattice shrinkage is consistent with the size differences between Ba^{2+} and Sr^{2+} ions. In fact, the radius of Ba^{2+} equals 1.35 Å, whereas that of Sr^{2+} equals 1.12 Å, implying that the substitution of Ba^{2+} for Sr^{2+} should introduce a noticeable lattice distortion, as observed by other researchers [21]. SEM images of $Ba_{1-x}Sr_xTi_{0.9}Sn_{0.1}O_3$ ($x = 0$, 0.06, 0.07, and 0.08) ceramics are shown in Fig. 2. All produced ceramics exhibited good quality. The average grain size among all samples equaled 10–20 μm. Sample densities were measured based on Archimedes' principle, equaling ~95% of the theoretical density and being in agreement with previously obtained values [6]. Thus, the fabricated ceramics were confirmed to be dense.

Table 1
Unit cell and positional and reliability factors for Rietveld refinements of $Ba_{1-x}Sr_xTi_{0.9}Sn_{0.1}O_3$ ($x = 0$, 0.06, 0.07, and 0.08) belonging to the tetragonal *P*4*mm* space group, as determined from XRD data; (*x*, *y*, *z* are coordinate axes, *Rwp* and *Rp* are agreement indices for Rietveld structure refinements, and χ is credibility).

x		0	0.06	0.07	0.08
a (Å)		4.0157(1)	4.0131(3)	4.0104(1)	4.0093(1)
c (Å)		4.0173(1)	4.0133(1)	4.0060(1)	4.0068(1)
V (Å^3)		64.78(1)	64.63(2)	64.43(1)	64.41(1)
Ba/Sr	*x*	1	1	1	1
	y	1	1	1	1
	z	1	−0.0522(3)	0.0008(6)	0.0016(2)
Ti/Sn	*x*	0.5	0.5	0.5	0.5
	x	0.5	0.5	0.5	0.5
	y	0.4385(1)	0.5178 (5)	0.4976(2)	0.5006(2)
O1	*x*	0.5	0.5	0.5	0.5
	y	0.5	0.5	0.5	0.5
	z	0.9723(1)	0.9653(2)	0.9838(1)	0.9893(5)
O2	*x*	0.5	0.5	0.5	0.5
	y	1	1	1	1
	z	0.6154(5)	0.5	0.5	0.5
Rwp		8.90%	9.96%	9.76%	8.15%
Rp		6.60%	7.05%	7.32%	5.98%
χ		1.26	1.31	1.14	1.42

Fig. 3 shows the temperature and frequency dependences of the dielectric permittivity of $Ba_{1-x}Sr_xTi_{0.9}Sn_{0.1}O_3$. For $x = 0$, T_c equaled 48.5 °C, in agreement with previously reported results [19]. The relationship between T_c and Sr content is displayed in the inset of Fig. 3a, revealing that T_c decreased with increasing Sr content. Since Sr^{2+} is smaller than Ba^{2+}, substitution of the latter for the former decreases the lattice volume (as confirmed by XRD results), which should reduce the potential energy and heat of phase transition, as demonstrated previously [20]. $Ba_{1-x}Sr_xTi_{0.9}Sn_{0.1}O_3$ ($x = 0.08$) displays a broad dielectric constant peak at T_c, indicating

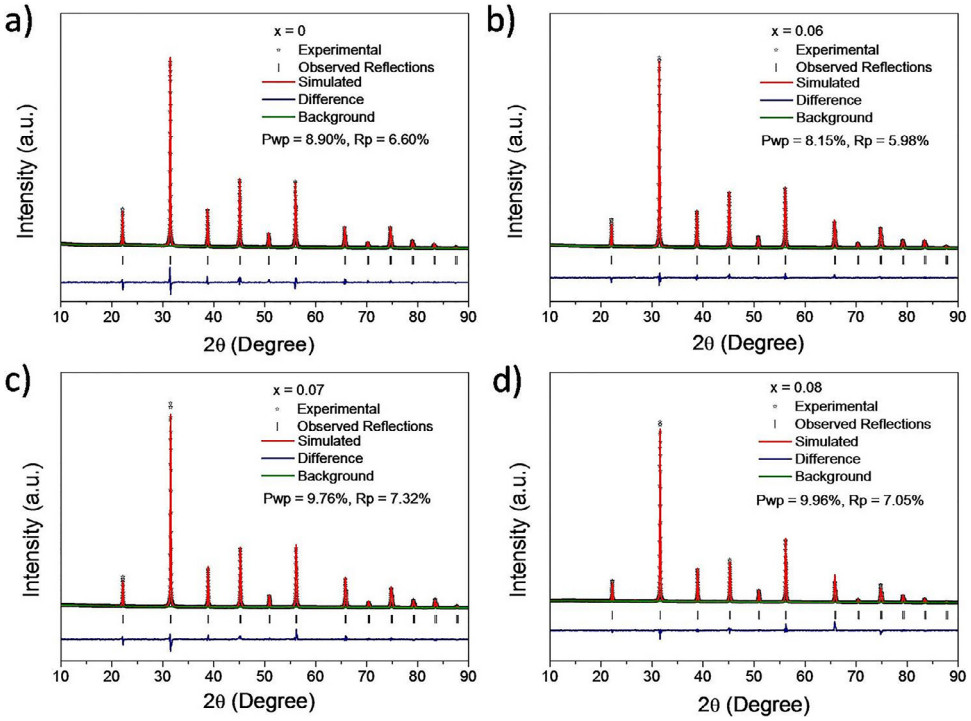

Fig. 1. Experimental, calculated, and difference XRD profiles for $Ba_{1-x}Sr_xTi_{0.9}Sn_{0.1}O_3$: (a) $x = 0$, (b) $x = 0.06$, (c) $x = 0.07$, and (d) $x = 0.08$.